THE JOURNAL OF BIOLOGICAL CHEMISTRY VOL. 292, NO. 7, pp. 2586–2600, February 17, 2017

Functional Transcriptomics in Diverse Intestinal Epithelial Cell Types Reveals Robust MicroRNA Sensitivity in Intestinal Stem Cells to Microbial Status*[S]

Received for publication, November 29, 2016, and in revised form, December 23, 2016 Published, JBC Papers in Press, January 4, 2017, DOI 10.1074/jbc.M116.770099

Bailey C. E. Peck[‡§1], **Amanda T. Mah**[¶], **Wendy A. Pitman**[§], **Shengli Ding**[‖], **P. Kay Lund**[‡¶‖], and **Praveen Sethupathy**[‡§2]

From the [‡]*Curriculum in Genetics and Molecular Biology,* [§]*Department of Genetics,* [¶]*Department of Nutrition, and* [‖]*Department of Cell Biology and Physiology, University of North Carolina at Chapel Hill, Chapel Hill, North Carolina 27599*

Edited by Xiao-Fan Wang

Gut microbiota play an important role in regulating the development of the host immune system, metabolic rate, and at times, disease pathogenesis. The factors and mechanisms that mediate interactions between microbiota and the intestinal epithelium are not fully understood. We provide novel evidence that microbiota may control intestinal epithelial stem cell (IESC) proliferation in part through microRNAs (miRNAs). We demonstrate that miRNA profiles differ dramatically across functionally distinct cell types of the mouse jejunal intestinal epithelium and that miRNAs respond to microbiota in a highly cell type-specific manner. Importantly, we also show that miRNAs in IESCs are more prominently regulated by microbiota compared with miRNAs in any other intestinal epithelial cell subtype. We identify miR-375 as one miRNA that is significantly suppressed by the presence of microbiota in IESCs. Using a novel method to knockdown gene and miRNA expression *ex vivo* enteroids, we demonstrate that we can knock down gene expression in Lgr5$^+$ IESCs. Furthermore, when we knock down miR-375 in IESCs, we observe significantly increased proliferative capacity. Understanding the mechanisms by which microbiota regulate miRNA expression in IESCs and other intestinal epithelial cell subtypes will elucidate a critical molecular network that controls intestinal homeostasis and, given the heightened interest in miRNA-based therapies, may offer novel therapeutic strategies in the treatment of gastrointestinal diseases associated with altered IESC function.

The intestinal epithelium is a single layer of cells exposed to the intestinal lumen and is composed of multiple cell types including the proliferative intestinal epithelial stem cells (IESCs)[3] and progenitor cells (also known as transit amplifying cells) as well as differentiated absorptive enterocytes and secretory goblet, Paneth, and enteroendocrine cells (EECs). IESCs divide to yield more rapidly proliferating progenitors that give rise to all of the other intestinal epithelial cell (IEC) types and drive continuous renewal of the intestinal epithelium every ~3–5 days (1). Proper renewal facilitates important intestinal epithelial functions including barrier integrity to protect against invasion of harmful toxins present in the intestinal lumen, nutrient digestion and absorption, and production of hormones that regulate systemic energy homeostasis. These physiological processes are mediated in part by interactions with resident microbiota (2). Studies using germ-free animals have demonstrated that gut microbiota influence intestinal barrier function, nutrient absorption, proliferation, differentiation, cellular signaling, and migration (3, 4). However, the molecular factors and mechanisms underlying microbiota-mediated control of IEC functions, particularly IESC proliferation, are unknown.

microRNAs (miRNAs) have emerged as critical regulatory factors of many biological processes in numerous tissues and are known to confer phenotypic robustness in response to environmental stimuli (5). However, less is known about miRNA expression and function in the intestinal epithelium compared with most other tissues. Recently, miRNAs were implicated in the regulation of IEC physiology (6, 7). McKenna *et al.* (6) demonstrated in mice that the IEC-specific knock-out of *Dicer1*, an essential enzyme for canonical miRNA biogenesis, results in altered IEC proliferation, differentiation, nutrient absorption, and impaired barrier function, indicating that miRNAs are likely important modulators of intestinal homeostasis (6). Furthermore, the presence of microbiota in the gut has been shown to alter miRNA expression profiles in intestinal macrophages

* This work was supported, in whole or in part, by National Institutes of Health Grants UNC GMB T32GM007092 (NIGMS), 5R25GM55336 (a UNC IMSD Diversity Fellowship; NIGMS to B. C. P.), F31DK105747 (NIDDK to B. C. P.), P30DK034987 (NIDDK; to P. S.), and R01DK105965 (NIDDK; to P. S.). This work was also supported by 14CSA20660001 (American Heart Association; to P. S.) and 1-16-ACE-47 (American Diabetes Association; to P. S.). The authors declare that they have no conflicts of interest with the contents of this article. The content is solely the responsibility of the authors and does not necessarily represent the official views of the National Institutes of Health.

[S] This article contains supplemental File 1.

Raw sequencing data and counts are available through GEO accession number GSE81126.

[1] To whom correspondence may be addressed: Curriculum in Genetics and Molecular Biology, School of Medicine, 5100H Genetic Medicine Bldg. CB#7264, 120 Mason Farm Rd., UNC Chapel Hill, Chapel Hill, NC 27599. E-mail: bpeck@email.unc.edu.

[2] To whom correspondence may be addressed: Dept. of Genetics, School of Medicine, 5091 Genetic Medicine Bldg. CB#7264, 120 Mason Farm Rd., UNC Chapel Hill, Chapel Hill, NC 27599. Tel.: 919-966-6387; E-mail: Praveen_sethupathy@med.unc.edu.

[3] The abbreviations used are: IESC, intestinal epithelial stem cell; miRNA, microRNA; IEC, intestinal epithelial cell; EEC, enteroendocrine cell; GF, germ-free; CV, conventionalized; EGFP, enhanced GFP; CR, conventionally raised; NS, non-sorted; RPMMM, reads per million mapped to miRNAs; PCA, principal component analysis; LNA, locked nucleic acid; FC, -fold change; FDR, false discovery rate; UNC, University of North Carolina at Chapel Hill; qRT, quantitative real-time; RQV, relative quantitative value.

(8) as well as in whole intestine (9, 10). Understanding the mechanisms by which microbiota regulate miRNA and gene expression in IESCs and other IEC subtypes will elucidate a critical molecular network that controls intestinal homeostasis and, given the heightened interest in miRNA-based therapies, may offer novel therapeutic strategies in the treatment of gastrointestinal diseases associated with altered IESC function. However, no study to date has investigated miRNA expression and activity across the functionally distinct IEC subtypes, and cell type-specific effects of microbiota on miRNAs is completely unknown. We hypothesized that each IEC population has a distinct miRNA profile and that miRNAs respond to gut microbiota in a cell type-specific manner in order to control function and overall homeostasis of the intestinal epithelium.

Results

Germ-free Mice Have an Altered Jejunal IEC Composition Compared with Their Conventionalized and Conventionally Raised Counterparts—We selected the well characterized Sox9-EGFP transgenic mouse model to evaluate miRNA expression and effect of microbiota in functionally distinct IECs. This model was originally created by GENSAT (11), who developed the model by randomly inserting into the mouse genome a BAC (bacterial artificial chromosome) containing the EGFP gene driven by the cloned genomic regions upstream and downstream of *Sox9* (12). A beneficial feature of this model is that EGFP expression is fully penetrant within the mouse intestine, which permits the isolation and analysis of four distinct IEC populations (12). Applying the same fluorescence-activated cell sorting (FACS)-based approach used to isolate IESCs from the commonly used Lgr5-EGFP model, which demonstrates mosaic expression among crypts in the intestine, both actively cycling IESCs ($Sox9^{Low}$) and transit-amplifying progenitor cells ($Sox9^{Sublow}$) can be isolated from the Sox9-EGFP mouse intestine (12, 13). Moreover, two additional differentiated cell populations can also be isolated on the basis of variable EGFP intensity, including $Sox9^{Neg}$ (mostly differentiated enterocytes as well as goblet cells and Paneth cells) and $Sox9^{High}$ (primarily EECs as well as reserve/quiescent +4 stem cells) (12–17).

To evaluate the effect of microbiota on miRNA expression in IECs, we first took a conventionalization approach (Fig. 1*a*). A 2-week conventionalization was selected because previous studies have shown this to be a time point at which the gene expression profile begins stabilizing in the small intestine of young mice after conventionalization (18–20). After generating germ-free (GF) Sox9-EGFP animals at the University of North Carolina at Chapel Hill (UNC) Gnotobiotic core facility, we selected four pairs of female GF Sox9-EGFP littermates from four different litters born between February and July 2015. One littermate from each pair was randomly selected at 8–10 weeks of age for conventionalization. The 2-week conventionalization resulted in a slightly decreased body weight relative to the remaining germ-free sibling along with a commensurate increase in liver weight (Fig. 2). However, no significant differences were observed in the length of the small intestine or colon between GF and conventionalized (CV) animals (Fig. 2). IECs were collected from the mid-region of the small intestine ("Experimental Procedures"), hereafter referred to as jejunum, of the GF and CV animals, and FACS was performed based on Sox9-EGFP intensity (Fig. 1*a*). Special care was taken to gate out cellular debris, dead and dying cells, immune cells, and multiplets during FACS (see "Experimental Procedures"; Fig. 3). Additionally, a strict gating scheme was used to avoid contamination between cell populations. To evaluate the accuracy of the sorting in our hands, we performed qRT-PCR on sorted cells from 10-week-old female conventionally raised Sox9-EGFP mice and demonstrated clear enrichment of *Chga* in the $Sox9^{High}$ population, *Lgr5* in the $Sox9^{Low}$ population, and *Mttp* in the non-sorted cells (which consists primarily of enterocytes) and the $Sox9^{Neg}$ population (Fig. 1*b*). As these genes are known to be enriched in EECs, IESCs, and enterocytes, respectively, these data confirm the utility and accuracy of the sorting method for isolating functionally distinct subpopulations of the intestinal epithelium.

Next we compared the abundances of each major IEC subpopulation in GF and CV animals to conventionally raised (CR) chow-fed animals. We found very similar abundances of $Sox9^{Sublow}$ cells (transit amplifying) and $Sox9^{Neg}$ cells (enterocytes, Paneth, and goblet) in CV and GF populations relative to CR mice (Fig. 1*c*). Notably, GF mice had significantly more $Sox9^{High}$ cells (EECs) than CR mice ($-$fold change $= 2.04$, $p = 0.04$; Fig. 1*c*), which is consistent with previous studies comparing EECs in the jejunum of GF and CR rodents (21, 22). Also, there were on average fewer $Sox9^{Low}$ cells (actively cycling IESCs) in GF mice relative to CR and CV mice, which has not been shown before but could help explain previous reports suggesting reduced proliferation in the small intestine of GF animals (20, 23–25).

IESCs Demonstrate Robust Transcriptional Differences between Distinct Microbial States—To evaluate the transcriptional changes that occur in response to conventionalization in the IESCs of GF and CV animals, we performed RNA sequencing analysis on the $Sox9^{Low}$ population (which we will refer to as IESCs for simplicity). We identified 823 genes and long, noncoding RNAs (lncRNAs) significantly elevated in GF IESCs and 334 genes and lncRNAs significantly elevated in CV IESCs (Fig. 4*a*). Gene Ontology Biological Process (26, 27) enrichment analysis using Enrichr (28) revealed that genes elevated in CV IESCs are most significantly overrepresented in pathways related to proliferation such as "mitotic cell cycle" and "nuclear division" (Fig. 4*b*). The genes elevated in GF IESCs genes were associated with processes related to hormone secretion and transport (Fig. 4*b*). Consistent with these findings, in CV IESCs we observed that established markers of proliferation (*Ccnb1*, *Cdk1*, and *Mki67*) were significantly up-regulated, positive transcriptional regulators of IESC proliferation and self-renewal (*Gata4* and *Gata6*) were up-regulated, and negative regulators of IESC proliferation and self-renewal (*Bmp4*) were down-regulated (Fig. 4*c*). Also, some, but not all, classic markers of EECs were up-regulated in GF IESCs (Fig. 4*c*), which could indicate some priming for cells to enter the EEC lineage, consistent with our observation that GF mice have more $Sox9^{High}$ cells. Known markers of reserve (quiescent) stem cells were not significantly different between CV and GF IESCs (Fig. 4*c*) nor were markers for Paneth cells (*Lyz*), goblet cells (*Muc2*),

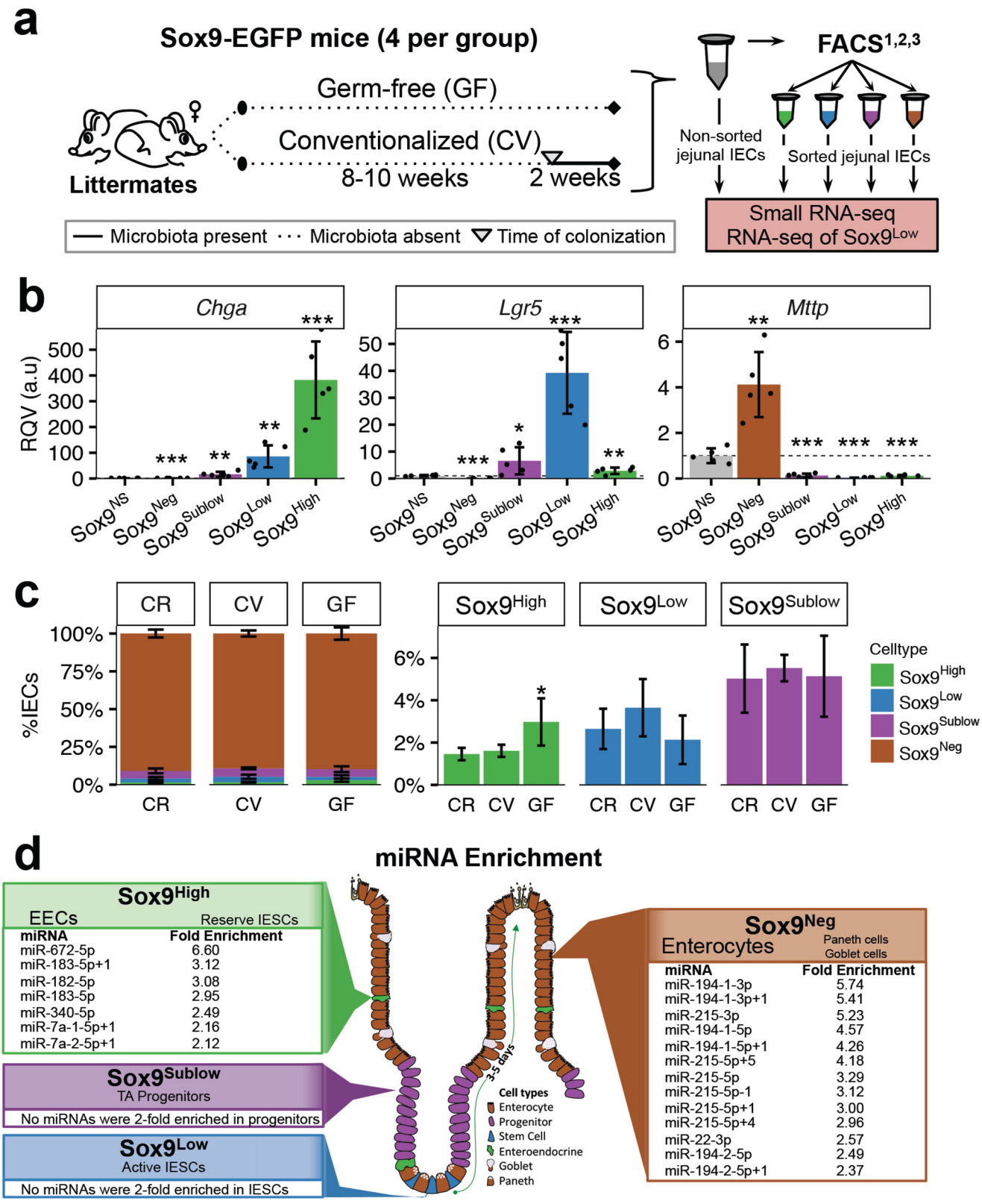

FIGURE 1. **The Sox9-EGFP mouse model for characterizing subpopulations of the mouse intestinal epithelium.** *a*, diagram of our experimental design. *b*, data from qRT-PCR analysis showing the normalized expression of *Chga*, *Lgr5*, and *Mttp* in sorted Sox9-EGFP populations relative to normalized expression in non-sorted cells ($Sox9^{NS}$) from 10-week-old CR female Sox9-EGFP mice ($n = 5$). Data are displayed as RQVs, which are in arbitrary units (*a.u.*). Significance was determined for each cell type in comparison to $Sox9^{NS}$ by Student's two-tailed unpaired *t* test and is denoted as: *, $p < 0.05$; **, $p < 0.01$; ***, $p < 0.001$. *c*, mean percentage of each IEC subtype sorted from jejunum of CR, GF, and CV mice ($n = 4$ each). Significance was determined for each category in comparison to CR by Student's two-tailed unpaired *t* test and is denoted as: *, $p < 0.05$. *d*, schematic showing location and types of IECs in the Sox9-EGFP mouse. Listed are miRNAs with a mean normalized expression (across CR, CV, and GF) that is at least 2-fold greater in one particular IEC subtype relative to all others. Only miRNAs with RPMMM > 400 in at least one sample were included in the analysis. *Error bars* depict S.D.

and enterocytes (*Elf3*). These data confirm that the Sox9^{Low} cells are indeed enriched for IESCs and that CV IESCs harbor a gene signature consistent with increased proliferative capacity. As miRNAs are known regulators of proliferation and differentiation, we performed small RNA sequencing of each of the functionally distinct IEC subpopulations from four CR, GF, and CV animals.

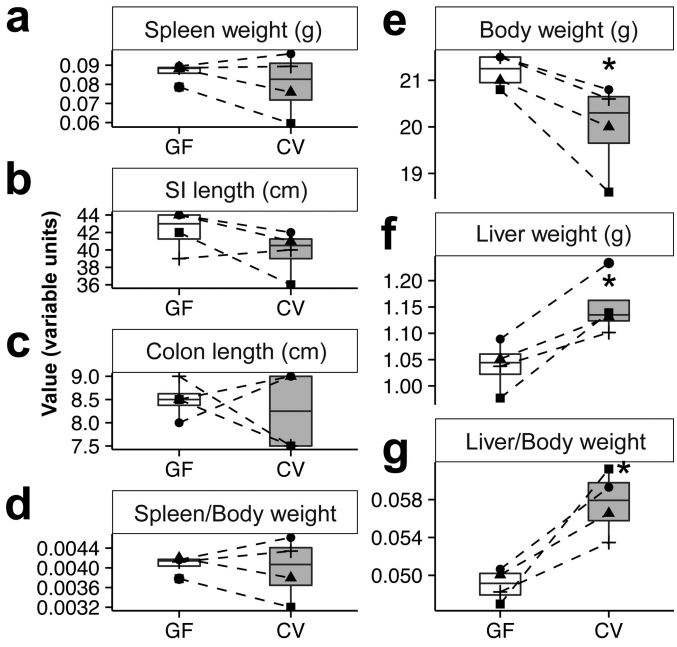

FIGURE 2. **Physiological parameters observed at the time of sacrifice of female GF and 2-week CV mice at 10–12 weeks of age ($n = 4$ each).** *a*, weight of spleen in grams. *b*, length of small intestine (*SI*) from pyloric sphincter to caecum in centimeters (cm). *c*, length of the colon from caecum to anus in cm. *d*, ratio of spleen weight to body weight (*BW*). *e*, body weight in grams. *f*, liver weight in grams. *g*, ratio of liver weight to body weight. Significance was determined by a Student's two-tailed paired *t* test is denoted as: *, $p < 0.05$.

miRNAs Show Cell Type-specific Expression across Functionally Distinct Populations of IECs—Total RNA was isolated from the four sorted populations from each animal as well as from non-sorted IECs (NS IECs; NS IECs were purified by FACS but not sorted based on Sox9-EGFP intensity). Small RNA-sequencing was performed in three batches, two of which contained small RNA libraries from sorted and unsorted IECs from two GF animals and two CV animals. The third batch contained libraries of the four CR animals. miRNAs and their isoforms (called isomiRs) were quantified using miRquant, our previously described method (see "Experimental Procedures" for details) (29). To test our hypothesis that miRNAs are differentially expressed among functionally distinct IEC subtypes, we evaluated miRNAs with an expression level of at least 400 reads per million mapped to miRNAs (RPMMM) in one or more samples, identifying 149 robustly expressed miRNAs across all IEC populations.

Many miRNAs were uniquely enriched in one IEC subtype relative to all others (>2-fold more highly expressed than any other cell type across all samples; Fig. 1*d*). For example, we found that miR-215 and miR-194 were enriched in Sox9^{Neg} cells, which consist primarily of enterocytes. Both of these miRNAs are processed from a single primary miRNA transcript on Chr1 and were previously shown to be induced by HNF4α during differentiation of Caco-2 colon carcinoma cells (30). Five miRNAs were enriched in Sox9^{High} cells (EECs and reserve stem cells) including miR-182–5p and miR-183–5p (Fig. 1*d*), which are also generated from a single primary miRNA transcript. Consistent with enrichment in a subpopulation of cells composed largely of EECs, miR-182 has been shown to have important functions in other endocrine cells, specifically, pancreatic beta cells (31). Unexpectedly, we did not find any miRNAs enriched in the Sox9^{Low} IESCs or Sox9^{Sublow} progenitors, which are the only actively proliferating cell populations (Fig. 1*d*).

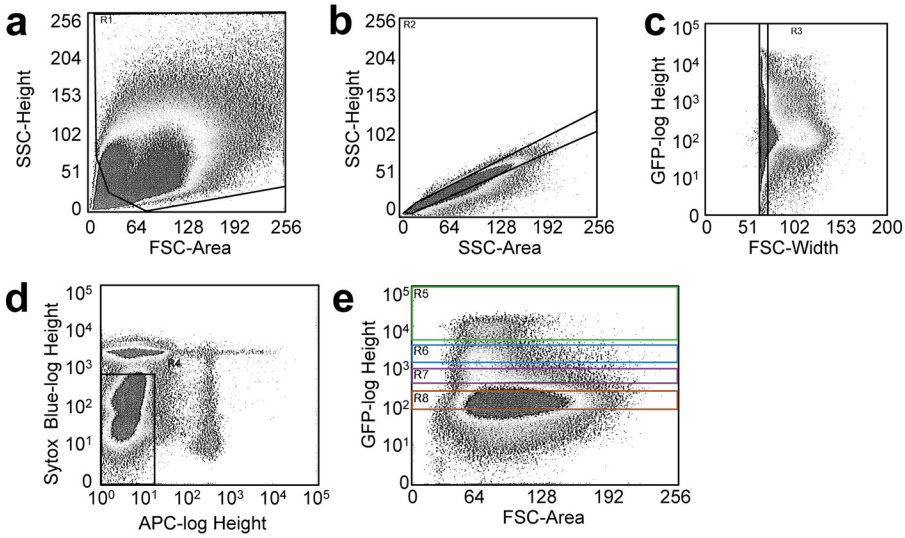

FIGURE 3. **Representative gating scheme for FACS of Sox9-EGFP IECs.** *a*, cells were gated to remove dead cells as well as cellular debris using side-scatter (*SSC*) height by forward scatter (*FSC*) area. *b* and *c*, singlets were selected for by gating on SSC-height by SSC-area and then FSC-width. *d*, dead and dying cells were gated out using Sytox blue and annexin V-APC staining, immune cells by CD45-APC staining, and endothelial cells by CD31-APC staining, leaving a highly pure IEC population for sorting based on EGFP intensity. *e*, distinct subpopulations of IECs were isolated based on their cellular EGFP intensity. Gating for GF and CV animals were set using a CR Sox9-EGFP animal. Representative sort images are from the sorting performed on IECs from one conventionalized mouse used in this study.

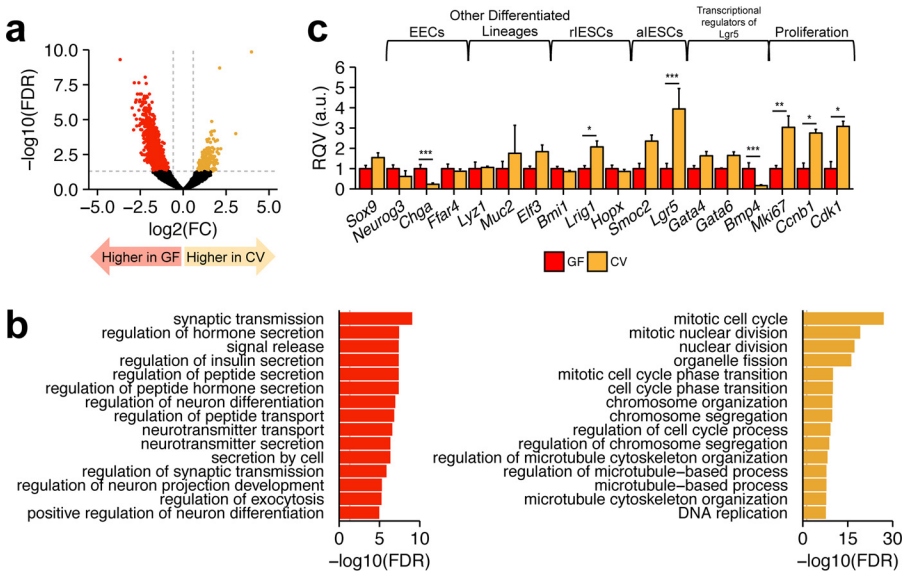

FIGURE 4. **RNA-seq analysis of the Sox9^{Low} population from GF and CV mice.** *a*, volcano plot showing differentially expressed genes in Sox9^{Low} IESCs between GF and CV mice ($n = 4$ animals per condition). The *horizontal dashed gray line* indicates a FDR of 0.05. *Vertical dashed gray lines* indicate FC = 1.5 and −1.5. Significantly differentially expressed genes are colored in *orange* and *red*, representing genes that at enriched in CV or GF IESCs, respectively. *b*, Top Enrichr Gene Ontology Biological Process enrichment terms for genes significantly up-regulated in GF (*left*) or CV (*right*) IESCs. *c*, RQVs, in arbitrary units (*a.u.*) of normalized counts for selected genes in CV relative to GF IESCs ($n = 4$ animals per condition), including markers of reserve or quiescent IESCs (rIESCs), and actively cycling IESCs (aIESCs). Significance determined using DEseq2 differential expression analyses is denoted as: *, FDR < 0.05; **, FDR < 0.01; ***, FDR < 0.001. *Error bars* depict S.D.

To further assess variability within and across samples, we performed principal component analysis (PCA) to reduce dimensionality and assess the effect of microbial presence on each sample. The first three principal components (PC1-PC3) captured 67% of the variability across samples. Using biplots, we evaluated segregation of samples by cell type and mouse condition (GF, CV, or CR). We showed that miRNA expression profiles were sufficient to cluster most samples by their respective cell types regardless of microbial status (Fig. 5, *a* and *b*). For example, Sox9^{Neg} cells and NS IECs were tightly clustered, which is expected given that NS IECs are composed of 85–90% Sox9^{Neg} cells. When we compared the samples using PC1 and PC2, GF Sox9^{Low} IESCs did not cluster together with CV and CR Sox9^{Low} IESCs (Fig. 5*a*), indicating that IESCs are particularly sensitive to the presence or absence of microbiota. However, when PC1 and PC3 were projected, clear cell type-specific clustering was observed regardless of mouse condition (Fig. 5*b*), suggesting that the subset of miRNAs loaded into PC2 (~40 miRNAs) contributed to the grouping observed in Fig. 5*a*. Taken together, these data indicate strong cell type-specific expression of miRNAs across IEC populations and a robust effect of microbial presence on the IESC population specifically. Both observations are supported by visualization of the most highly expressed miRNAs across GF and CV samples (Fig. 5*c*).

miRNAs of IESCs Show More Distinct Expression Differences between GF and CV States Than Other IEC Types—To evaluate the cell type-specific sensitivity to microbial status and to account for batch and littermate effects, we used a linear modeling approach (see "Experimental Procedures"). We found the expression levels of 11 miRNAs (miR-34a-5p, miR-200c-3p, miR-200c-3p-1, miR-143-3p, miR-130b-3p, miR-140−3p+1, miR-378−3p+1, miR-20a-5p, miR-17-5p, miR-93-5p, and miR-29a-3p) to be significantly influenced by microbial status across all cell populations. These miRNAs in general were elevated in CV mice across all cell populations, although the magnitude of the effect was always most pronounced in the Sox9^{Low} (IESC) population. When we assessed changes specific to each cell type, we were surprised to find that although many miRNAs were altered significantly in the IESC population in the CV state relative to GF, no miRNAs were identified as significantly changed specifically in the Sox9^{High}, Sox9^{Sublow}, or Sox9^{Neg} populations (Fig. 6*a*, supplemental File 1). A total of 19 miRNAs in IESCs were significantly different in expression depending on microbial status (Fig. 6*b*). This finding underscores the highly cell type-specific effect of microbial presence on miRNAs.

Of these 19 microbiota-sensitive miRNAs in IESCs, miR-375-3p was ~2.5-fold (false discovery rate (FDR) = 0.003) reduced in CV IESCs compared with GF IESCs and was the most highly expressed (Fig. 6, *a* and *b*). Notably, miR-375-3p was 2.4- and 7.2-fold more highly expressed than the next-most significant microbiota-sensitive miRNA in the CV and GF IESC populations, respectively (Fig. 6*b*). We also found that its isomiRs, miR-375-3p-1 and miR-375-3p+1, were also both significantly down-regulated in IESCs upon conventionalization ((−fold change (FC) = −2.45, FDR = 0.0006; FC = −2.47, FDR = 0.02, respectively; Fig. 6*b*). qRT-PCR on Sox9^{Low} cells confirmed that the miR-375-3p family was significantly down-regulated by conventionalization (FC = −3.85, $p = 0.03$; Fig. 6*c*). Of note, miR-375-3p exhibited rather low expression in Sox9^{Sublow} progenitors and Sox9^{Neg} cells (Fig. 6*d*). Although miR-375-3p is highly expressed in Sox9^{High} EECs, it was not altered in EECs by conventionalization and was only significantly down-regulated by microbiota in the IESCs.

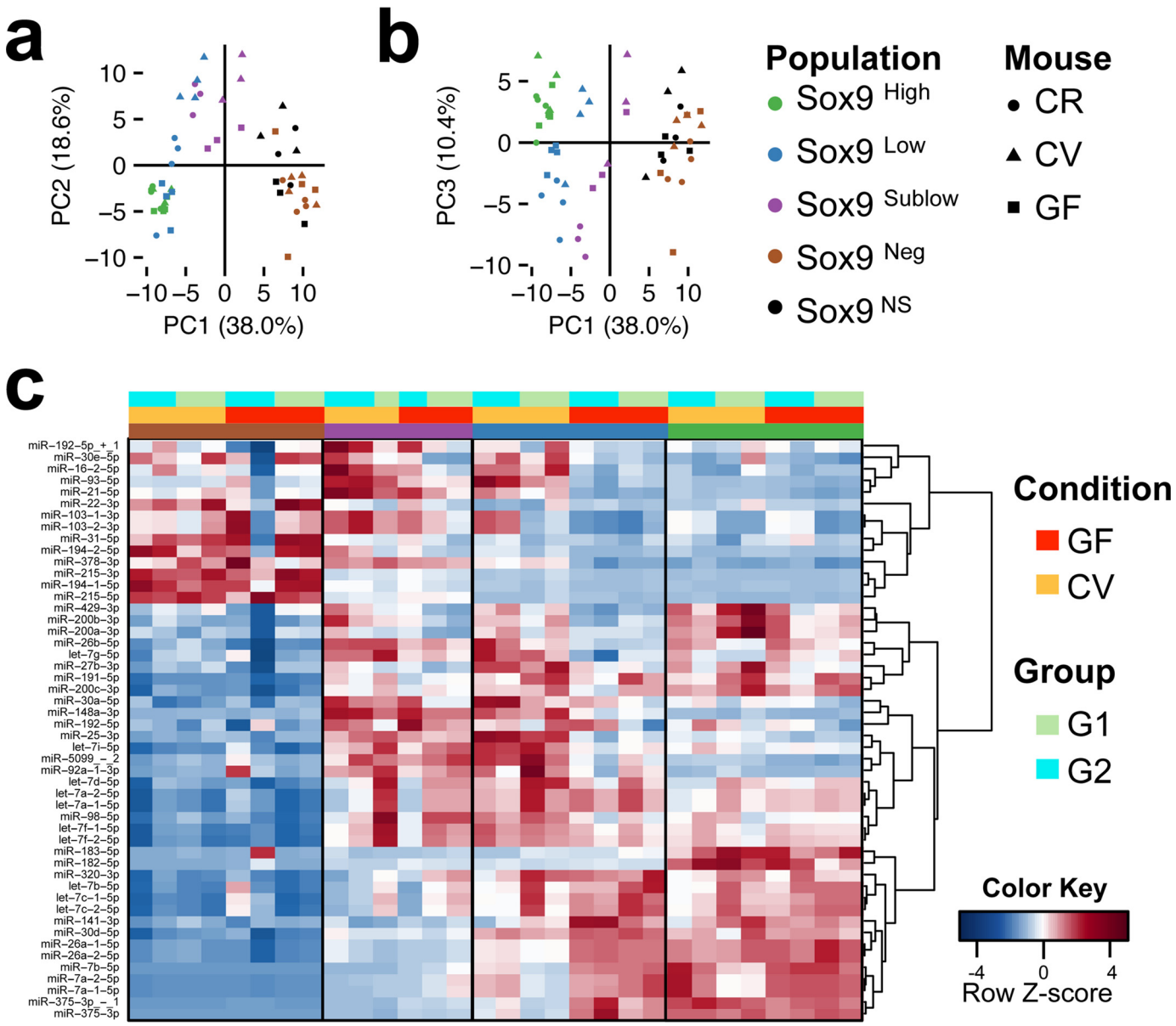

FIGURE 5. **miRNAs in the intestinal epithelium showed cell type-specific expression and sensitivity to microbial status.** *a* and *b*, PCA applied to miRNA expression for all miRNAs that reached an expression threshold of at least 400 RPMMM in 1+ samples ($n = 149$). Biplots of variance projections of PC1 on PC2 (*a*) and PC1 on PC3 (*b*) are shown. Percent variance explained by each principal component is shown in *parentheses along each axis*. Samples are colored based on the cell population, and the shape of the point indicates whether the sample came from a CR, GF, or CV mouse. *c*, hierarchical clustering of the top 50 most highly expressed miRNAs across sorted intestinal epithelial cell populations across all categories of mice. *Color bars* denote cell population, condition, and sequencing group (G1 or G2). Within the heatmap, *red* represents the high end of the expression spectrum, and *blue* represents the low end.

Knockdown of Gene Expression in IESCs of ex Vivo Enteroids using Gymnosis—To functionally evaluate the effect of the observed miRNA and gene expression changes, we sought out methods to suppress miRNA/gene expression in IESCs of *ex vivo* enteroid culture systems, which have been shown to maintain *in vivo* cellular composition and molecular gene expression profiles over time (32). We evaluated the use of gymnosis, a term coined by the Troels Koch laboratory in 2009 (33), to describe a process of introducing modified or locked nucleic acids (LNA) complementary to a specific gene or miRNA into cells without the use of traditional transfection reagents. Gymnosis has been used previously to knockdown gene expression in enteroids (34); however, knockdown capacity specifically in IESCs has not been evaluated. To determine whether IESCs of *ex vivo* cultured enteroids can take up LNAs introduced through the media and/or Matrigel via gymnosis and down-regulate target gene/miRNA expression (Fig. 7*a*), we tested knockdown efficacy of an LNA against EGFP (LNA-EGFP) in Lgr5-EGFP$^+$ enteroids. Specifically, we identified EGFP$^+$ crypts immediately after seeding into Matrigel and followed the growth of those enteroids over the course of 8 days and measured the EGFP signal after 1 μM LNA-EGFP treatment (Fig. 7, *b*–*e*). As Lgr5-EGFP crypts exhibit mosaic expression of EGFP (in our colony, ~1 in 30 crypts are EGFP$^+$), qRT-PCR analysis to assess changes in *EGFP* was inconclusive (data not shown). However, based on fluorescence imaging, we observed an appreciable depletion of EGFP by day 4 (Fig. 7*b*). We also demonstrated that knockdown efficiency improved with repeated

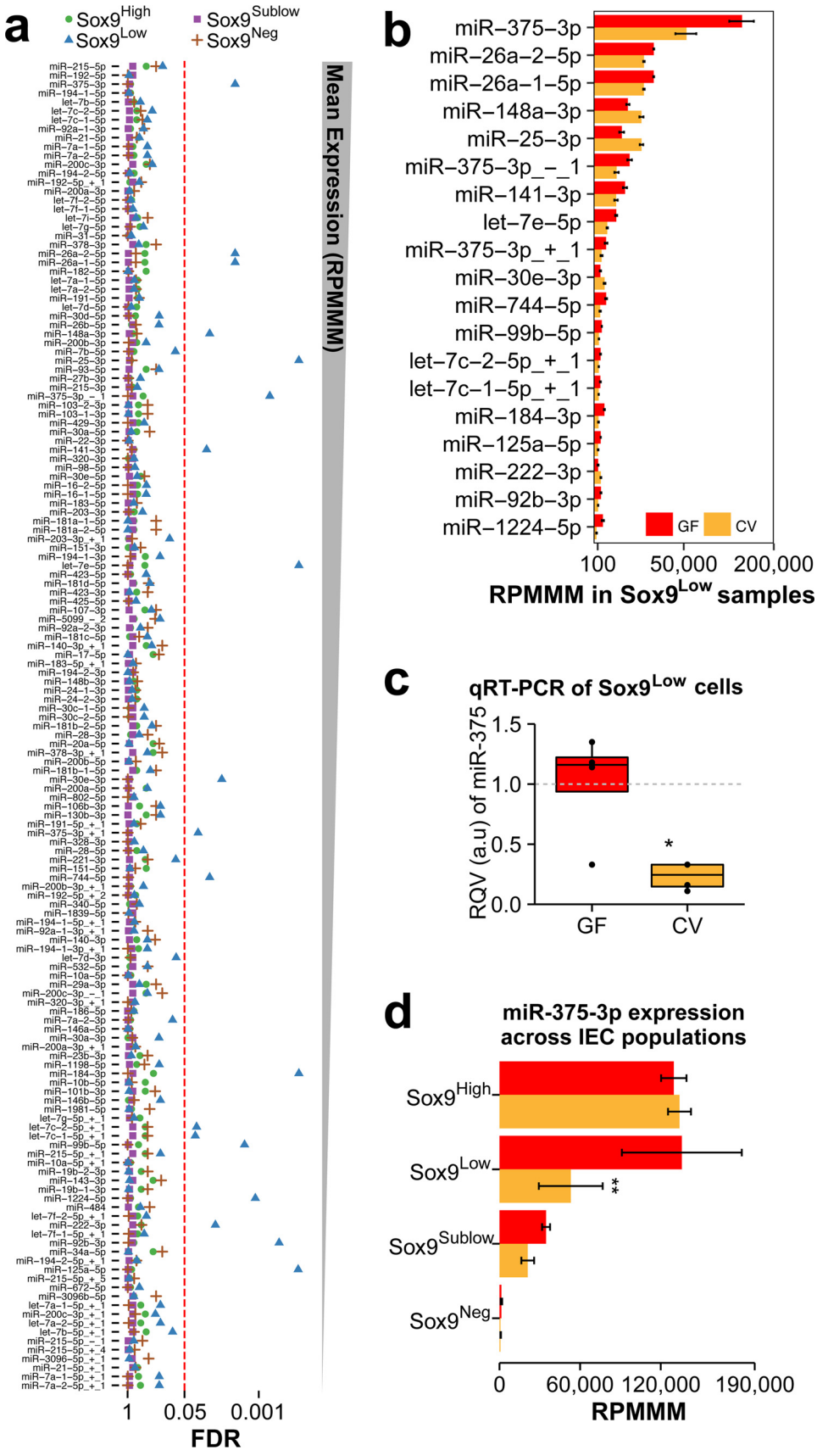
a
Sox9High
Sox9Low
Sox9Sublow
Sox9Neg
Mean Expression (RPMMM)
1
0.05
0.001
FDR
b
miR–375–3p
miR–26a–2–5p
miR–26a–1–5p
miR–148a–3p
miR–25–3p
miR–375–3p_–_1
miR–141–3p
let–7e–5p
miR–375–3p_+_1
miR–30e–3p
miR–744–5p
miR–99b–5p
let–7c–2–5p_+_1
let–7c–1–5p_+_1
miR–184–3p
miR–125a–5p
miR–222–3p
miR–92b–3p
miR–1224–5p
GF
CV
100
50,000
200,000
RPMMM in Sox9Low samples
c
qRT-PCR of Sox9Low cells
RQV (a.u) of miR-375
1.5
1.0
0.5
0.0
*
GF
CV
d
miR-375-3p expression across IEC populations
Sox9High
Sox9Low
Sox9Sublow
Sox9Neg
**
0
60,000
120,000
190,000
RPMMM

LNA-EGFP treatment over time (Fig. 7*c*). Moreover, whereas 1 μM and 5 μM concentrations of LNA-EGFP were sufficient to achieve considerable knockdown of EGFP, a 500 nM concentration was not, indicating a clear dose-dependent effect (Fig. 7*d*). Finally, as there are multiple enteroids per well, we sought to assess the level of within-well variability of the knockdown efficiency by surveying all $EGFP^+$ crypts from a single well treated with LNA-EGFP. Overall, EGFP knockdown efficiency appeared to be high across all of the $EGFP^+$ enteroids that were visualized (Fig. 7*e*). Taken together, these data indicate successful LNA-mediated knockdown of *EGFP* gene expression in IESCs of *ex vivo* Lgr5-EGFP enteroids using gymnosis and support the general use of gymnosis for knockdown of gene expression in IESCs of enteroids.

Knockdown of miR-375-3p in Enteroids Results in Increased Proliferation—To test the functional effect of miR-375-3p suppression, we knocked-down miR-375-3p by gymnosis in enteroids from GF Sox9-EGFP crypts. We achieved a robust ~700-fold knockdown of miR-375-3p at day 8 after treatment with an LNA inhibitor of miR-375-3p (LNA-375; Fig. 8*a*). At both days 4 and 8, LNA-375-treated enteroids exhibited significantly increased budding (Fig. 8, *b* and c), a marker of IESC proliferative capacity (35, 36), relative to Mock or enteroids treated with a scrambled LNA (LNA-SCR). This finding was confirmed when the experiments were repeated in enteroids established from crypts isolated from conventionally raised Lgr5-EGFP (Fig. 8*d*) and wild-type C57BL/6J mice (Fig. 8*e*). Consistent with this finding, whole mount staining of the enteroids also showed increased signal for Ki67 upon knockdown of miR-375-3p (Fig. 8*f*), although no difference in enteroid size (Fig. 8, *g* and *h*) or passage efficiency was observed (data not shown). These data indicate that miR-375-3p is likely a potent regulator of IESC proliferation and that microbiota may regulate IESC renewal in part via modulation of miR-375-3p (Fig. 9).

Discussion

In this study we provided novel evidence that miRNAs are sensitive to the presence of gut microbiota in a cell type-specific manner. Microbiota exert the strongest effect on host miRNA expression in the $Sox9^{Low}$ population, which is highly enriched in IESCs (12–14, 16, 17). Subpopulation analysis was necessary to identify this effect, as IESCs make up only 1–3% of all IEC types. miR-375-3p was identified as significantly down-regulated in the IESC population in response to microbial presence, and follow-up experiments *ex vivo* demonstrated miR-375-mediated control of IESC expansion and proliferation, thereby providing a mechanism by which microbiota may regulate these processes during conventionalization *in vivo*. miR-375-3p has been associated previously with the regulation of proliferation and differentiation in several tissues (34, 38, 39). It is predicted to target many members of the Wnt/β-catenin and Hippo signaling pathways but so far has only been experimentally shown to directly inhibit Frizzled-8 (39) and Yap1 (40). miR-375-3p has been knocked down systemically in mice, and although the authors did not study intestinal proliferation, they observed an increased rate of intestinal transit (41). miR-375-3p is best studied in the context of pancreatic endocrine cell differentiation and function (42–44), and more recently, Knudsen *et al.* (34) identified a role for miR-375-3p in regulating EEC differentiation as well. We found that although miR-375-3p is robustly expressed in both IESCs and EECs, it is sensitive to microbiota only in IESCs (Fig. 6*d*). This observation might suggest cell type-specific microbial signaling pathways and cell type-specific roles for miR-375-3p.

Our RNA sequencing analysis, the first to our knowledge comparing GF and CV IESCs, demonstrates substantial gene expression differences in IESCs between the GF and CV states. CV IESCs showed up-regulation of genes associated with proliferation. Of note, our data indicate a ~4-fold increase in *Lgr5* mRNA expression (Fig. 4*c*). Microbiota may regulate Wnt signaling upstream of Lgr5, an R-spondin ligand receptor, as known upstream regulators of Lgr5 are also altered by the presence of microbiota, including *Gata4*, *Gata6*, and *Bmp4* (Fig. 4*c*) (45, 46). This is a finding that deserves further investigation.

An unexpected finding was that GF IESCs ($Sox9^{Low}$) have a gene and miRNA expression profile demonstrating some similarity to $Sox9^{High}$ cells. Given the careful sorting protocol and the observation that $Sox9^{High}$-enriched genes and miRNAs change in both the upward and downward directions within the $Sox9^{Low}$ population, our finding is unlikely to be driven solely by contamination between populations. One possible explanation is that $Sox9^{Low}$ cells are primed for the EEC lineage in the absence of microbial influence. Alternatively, one of the caveats of the Sox9-EGFP model is that although the $Sox9^{High}$ populations consist primarily of EECs, they also include a small population of reserve stem cells (17). It is, therefore, possible that microbiota influence the maintenance of reserve stem cells in addition to their role in regulating actively cycling IESCs through miR-375-3p, although the gene expression data do not fully support this hypothesis. Although outside the scope of this study, more research including single cell analyses will need to be conducted to delineate more precisely the differences between GF and CV IESCs as well as to determine which miRNAs are involved in the maintenance of active and quiescent IESC states.

An important added value of our study is the first ever map of miRNA expression across different IEC subtypes and the cell type-specific influence of microbial conventionalization on

FIGURE 6. **Cell population-specific differences in miRNA expression between GF and CV revealed through linear modeling analysis.** *a*, for each miRNA that met an expression threshold of RPMMM >400 in 1+ samples, the FDR of the cell population condition covariate interaction *p* value of our linear model analysis is plotted. miRNAs are ordered by average expression across all IEC subtypes across all categories (GF, CV, and CR), and the *vertical red dashed line* indicates FDR = 0.05. Cell population is signified by color and shape. *b*, the mean RPMMM of the 19 miRNAs identified as significant (FDR < 0.05) in the $Sox9^{Low}$ population (in *panel a*) are plotted for both GF and CV mice ($n = 4$ each). The *x* axis is shown on a square root scale. *c*, qRT-PCR data confirming sequencing results for miR-375 expression in the $Sox9^{Low}$ population from CV and GF mice ($n = 4$ for each condition). Data are shown in a standard *box-and-whisker plot* with the median displayed as a *thick horizontal line*, the *shaded region* depicting the inner quartile range (IQR), and whiskers extending to the maximum and minimum data points that fall within 1.5× IQR. * $p < 0.05$, two-tailed Student's *t* test. *a.u.*, arbitrary units. *d*, Mean RPMMM of miR-375 in each cell population is shown for both GF and CV mice ($n = 4$ each). Error bars depict S.D.

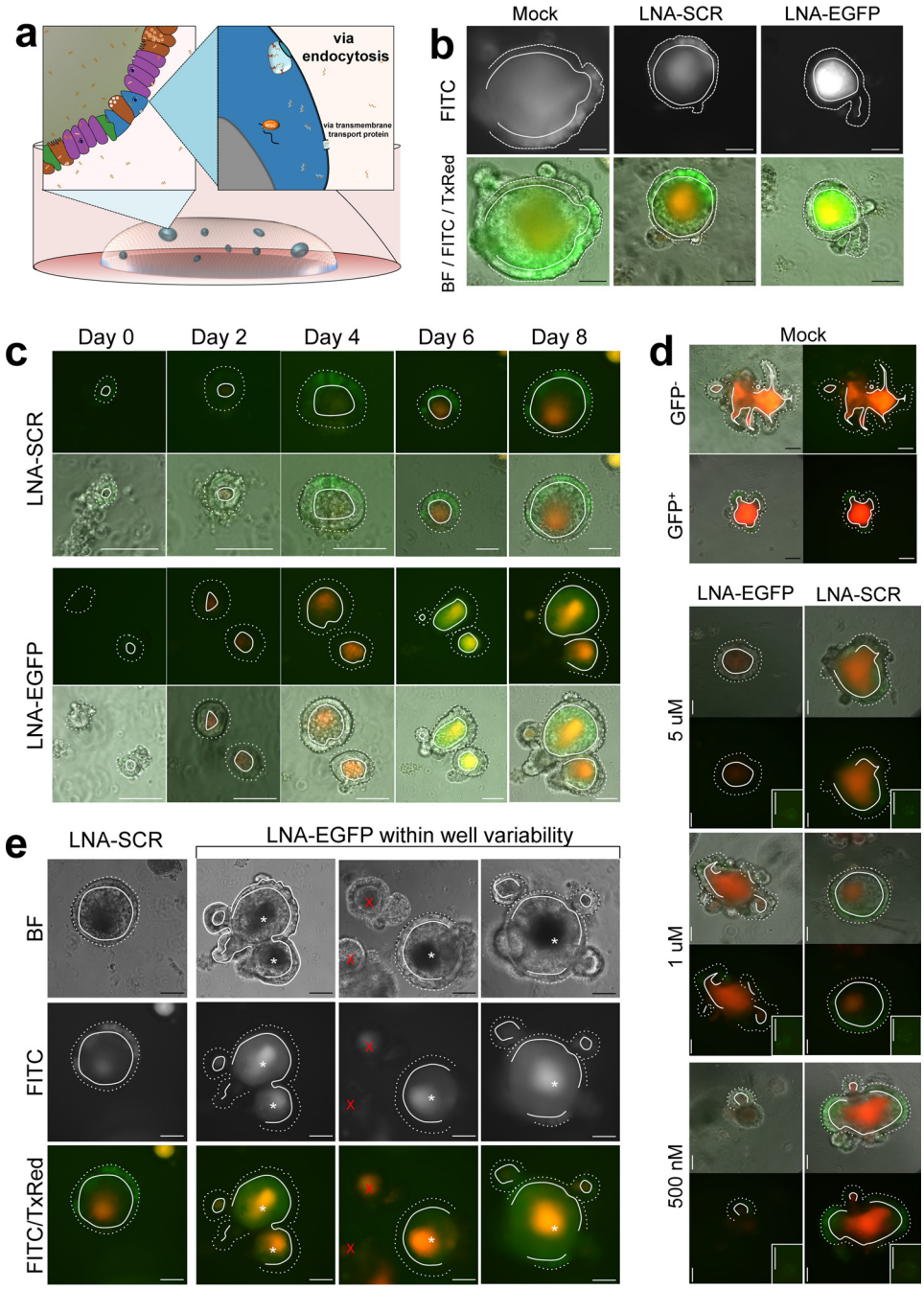

FIGURE 7. **Gymnosis was effective for knocking down gene expression in Lgr5-EGFP$^+$ stem cells.** *a*, schematic of miRNA knockdown in enteroids using gymnosis. *b*, representative images of EGFP$^+$ enteroids identified at day 0 and tracked over the course of 8 days using fluorescence microscopy are shown after gymnosis using no LNA (*Mock*), 1 μM LNA-SCR, or 1 μM LNA-EGFP. FITC alone (*top*), stacked Bright Field (*BF*), FITC, and TxRed image (*bottom*). *c*, time course of EGFP$^+$ enteroids treated with 1 μM LNA-SCR or 1 μM LNA-EGFP. *d*, level of knockdown of EGFP in EGFP$^+$ enteroids 8 days after treatment with three different concentrations of LNA-EGFP or LNA-SCR (5 μM, 1 μM, and 500 nM). An example of an EGFP$^-$ enteroid is included from a Mock-treated well. *Top corner insets* show enteroids at day 0 confirming positive EGFP expression. *e*, all EGFP$^+$ enteroids from one well of LNA-EGFP treated enteroids are shown at day 8. EGFP$^-$ enteroids within the frame are marked with a *red x*. *b–e*, unless otherwise indicated, images shown in each panel for each treatment condition are from: *i*, FITC/TxRed stacked fluorescence image; *ii*, stacked Bright Field (*BF*), FITC, and TxRed (merged) image. TxRed is used to estimate autofluorescence, commonly observed in the enteroid center. In all images, *dashed* and *solid white lines* indicate the region within the image that has minimal projection into the z-frame (focused). FITC signal in between *dashed* and *solid lines* was used to determine EGFP knockdown efficacy.

miRNA expression. We also provide evidence that IESC microbiota-sensitive miR-375-3p influences IEC proliferation, most likely through physiological maintenance of actively cycling IESC. Of course many questions still remain, including how microbiota influence miRNA expression in IESCs. This phenomenon may be explained by direct and/or indirect mechanisms. Regarding the former, although thus far bacteria have only been found to reside within the crypts of the caecum and colon, where microbial density is highest (47), it nevertheless remains a possibility that bacteria residing within the jejunal crypt may directly influence miRNAs in the stem cell subpopulation. Indirect mechanisms are also possible, such as changes

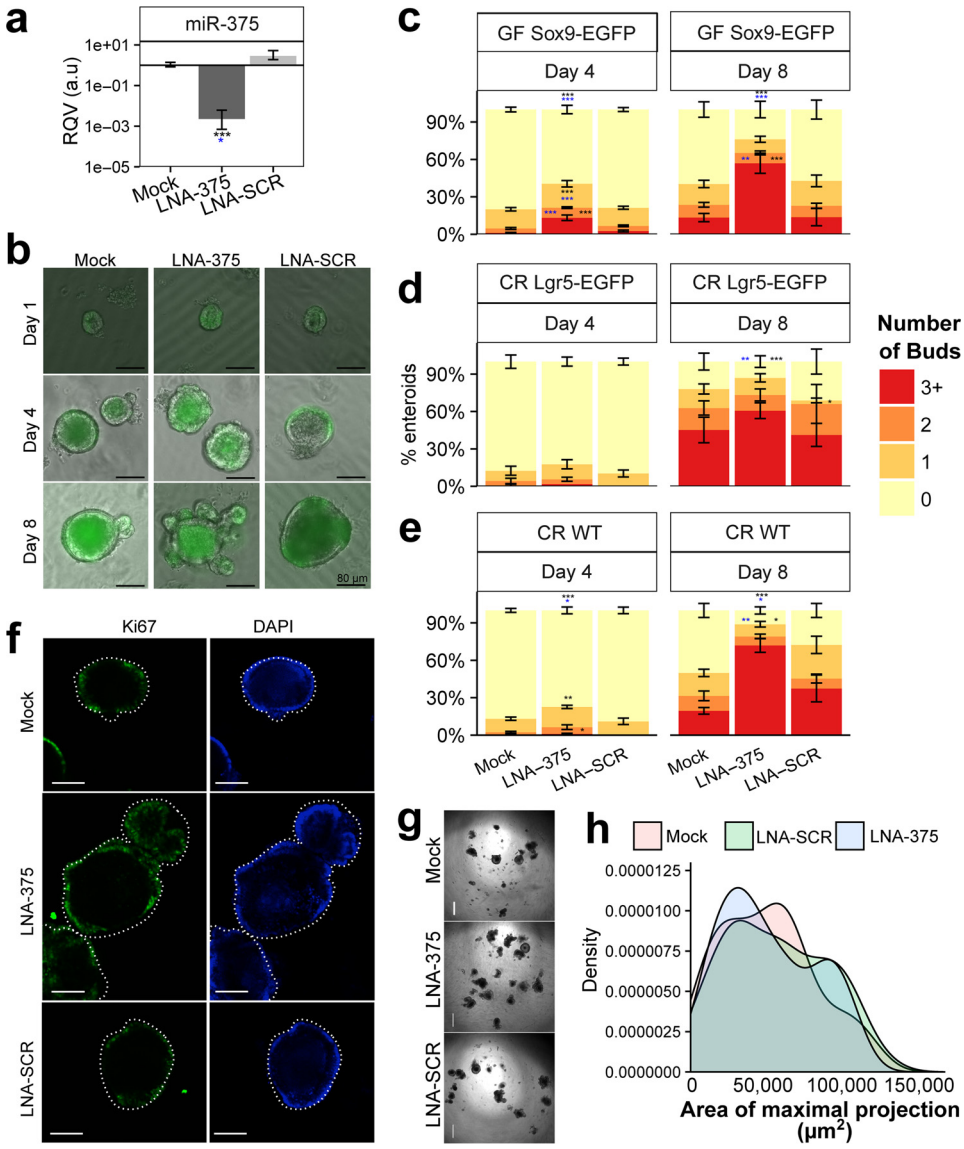

FIGURE 8. ***Ex vivo* knockdown of miR-375 using gymnosis in enteroids resulted in increased proliferation.** *a*, RQVs are shown for miR-375-3p in Mock-, LNA-375-, and LNA-SCR-treated enteroids from female GF Sox9-EGFP mice at day 8 as measured by qRT-PCR. *Error bars* reflect S.D. *a.u.*, arbitrary units. *b*, representative images at day 1, day 4, and day 8, after treatment with no LNAs (Mock), LNA-375, or LNA-SCR (enteroids shown are from the same experiments for which quantitative data are shown in *panels a* and *c*). Sox9-EGFP expression (FITC/*green*) is overlaid on the bright field images. *c–e*, mean percent of enteroids with 0, 1, 2, or 3+ buds at day 4 and day 8 after treatment with no LNAs (Mock), 500 nM LNA-375, or 500 nM LNA-SCR are shown for enteroids generated from female GF Sox9-EGFP mice (mock, $n = 12$; LNA-375, $n = 11$; LNA-SCR, $n = 9$) (*c*), male Lgr5-EGFP mice (mock, $n = 7$; LNA-375 $n = 6$; LNA-SCR, $n = 6$) (*d*), and female wild-type C57BL/6J mice (mock, $n = 16$; LNA-375, $n = 16$; LNA-SCR, $n = 12$) (*e*). *f*, confocal images of whole mount enteroids stained for Ki67 and DNA (DAPI). *g*, representative 4× images of wells from the same experiments represented in *panel c* are shown. *h*, distribution of enteroid sizes (μm^2) from one experimental replicate from *panel d* ($n = 3$ wells each). Experiments were performed in duplicate or triplicate unless noted. The *n* refers to number of wells. Significance determined by a Student's two-tailed unpaired *t* test relative to Mock (*black asterisks*) or LNA-SCR (*blue asterisks*) are denoted as: *, $p < 0.05$; **, $p < 0.01$; ***, $p < 0.001$. *Scale bars* depict 80 μm.

in the microenvironment (metabolites and bacterial endotoxins) or through indirect signaling by immune or mesenchymal cells, which were not profiled in this study. Although outside the scope of this analysis, further research is certainly warranted to investigate the interesting relationship between host miRNAs and resident microbiota.

It is also reasonable to consider in future studies how changes in miRNA expression in IESCs or other cell populations in response to environmental stimuli may in turn directly or indirectly influence gut microbial load and/or composition. As IESCs give rise to all IEC types, small changes in miRNA expression in these cells may result in altered intestinal epithelial composition. We have already shown in a previous publication that manipulation of a single miRNA promotes enterocyte differentiation (48), and it is likely that other miRNAs influence the differentiation of other IEC types. A change in relative number or secretions of secretory cells, including goblet and Paneth cells, could affect the composition of the gut microbiome (49–51). Of note, miRNAs can be loaded into the extracellular vesicles that are secreted both basolaterally and apically into the lumen (52). A recent study suggests that these luminally located miRNAs may regulate the composition of the gut microbiome (53). Investigating the mutual regulatory relationship between resident microbiota and host intestinal epithelial

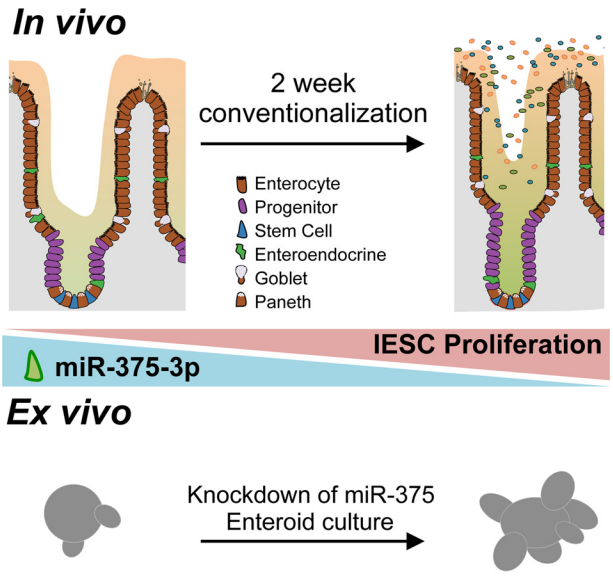

FIGURE 9. **Current working model of miR-375-3p-mediated effects of microbiota on IESC proliferation.** Previous research shows increased intestinal epithelial proliferation upon conventionalization of GF mice. We found that miR-375-3p is down-regulated in IESCs from CV mice relative to GF mice and that *ex vivo* knockdown of miR-375-3p in enteroids results in increased proliferative capacity.

miRNAs is of substantial interest and potential therapeutic relevance.

It is important to note that each segment of the intestinal epithelium has distinct physiological roles and differing magnitudes of microbial load. Our study only examined changes in response to microbial presence in IECs from the mid-section of the small intestine (which we referred to as jejunum throughout for simplicity). In the future it would be important to assess differences in cell type-specific responses to microbiota along the entire length of the intestine. Additionally, it would be interesting to investigate cell type-specific responses to microbiota in other populations not sorted herein, including goblet and Paneth cell populations. These cell types do not express Sox9-EGFP and are rare cell populations in the $Sox9^{Neg}$ fraction, which is composed primarily of enterocytes. Nevertheless, Paneth and goblet cells may experience robust changes in response to microbial presence based on their known functions. Although our current study focuses on the Sox9-EGFP model, which precluded examining these populations, they deserve attention in future work.

From an experimental standpoint, our study also provided validation of an important new tool to knock down gene expression in IESCs of intestinal enteroids using gymnosis, a technique that does not rely on cytotoxic transfection reagents (33, 34). Although not fully investigated in this study, it is possible that gymnosis allows for the uptake of LNAs into other IEC types in addition to IESCs. In one of our previous studies of an intestinal cell line we demonstrated stable knockdown of target miRNAs for 21 days after a single LNA transfection (48), which highlights the remarkable stability of LNAs in culture. Further investigation of the stability of LNAs in enteroids as well as the knockdown efficacy in other IEC types is warranted to evaluate the full utility of this assay. Nevertheless, because knockdown of gene expression in IESCs has proven quite difficult, requiring electroporation and adenoviral mediate knockdown, this study presents a quick and affordable alternative to knockdown gene and miRNA expression in IESCs of enteroids.

Conclusions

In summary, we provide novel data on the miRNA landscape in four distinct cell populations from the intestinal epithelium and demonstrate that miRNA profiles are very different across the IEC subtypes and also that miRNA sensitivity to microbial status is highly cell type-specific. IESCs demonstrate robust gene and miRNA expression changes at 14 days post-conventionalization. We investigate one IESC microbiota-sensitive miRNA, miR-375-3p, and show that its suppression in *ex vivo* enteroids results in significantly increased proliferative capacity, providing one possible mechanism by which microbiota regulate proliferation of IESCs *in vivo*. We believe the data provided herein progress the field and provide the scientific community a valuable resource through which researchers can initiate novel studies into miRNAs and microbiota-mediated regulation of intestinal physiology, homeostasis, and disease pathogenesis.

Experimental Procedures

Animals—All animal studies were approved by the University of North Carolina at Chapel Hill's Institutional Animal Care and Use Committee. The original source and maintenance of *Sox9-EGFP* mice have been described elsewhere (12–14). GF Sox9-EGFP mice on a C57BL/6J background were generated at the UNC Gnotobiotic Core Facility. Four pairs of female GF littermates were used in these experiments at 8–10 weeks of age. Each pair came from separate litters born between April and July 2015. GF mice were housed with animals of the same sex from the same litter on Envigo 7070C Tekland Diamond Dry Cellulose bedding. Four age-matched conventionally raised Sox9-EGFP animals and wild-type C56BL/6J animals were included as controls in each individual FACS experiment. Conventionally raised and conventionalized mice were bedded on Andersons irradiated ¼-inch Bed-O'cobs laboratory animal bedding. The small RNA-seq data presented for conventionally raised animals was generated in a separate experiment, which isolated each IEC population from female conventionally raise animals fed a standard chow diet at 30-weeks of age. The qRT-PCR data presented in Fig. 1*b* were generated using FACS-isolated cells (described below) from five 10-week-old female conventionally raised animals. Crypt culture studies were performed using female conventionally raised C56BL/6J, female GF Sox9-EGFP animals, and male conventionally raised Lgr5-EGFP-IRES-creERT2 mice. Conventionally raised animal colonies were maintained several generations at the University of North Carolina at Chapel Hill.

Conventionalization—For each littermate pair, 0.2–0.7 g of fresh fecal pellets were collected on separate days from multiple animals across 6–8 cages in the conventionally raised Sox9-EGFP animal colony housed at UNC and were frozen at −80 °C until reconstitution. Less than 1 h before conventionalization, the fecal sample was thawed on ice and then reconstituted at 1 g/10 ml cold PBS under anaerobic conditions. The fecal slurry was passed through a 100-μm filter to remove debris, and 1 ml

was aliquoted into a fresh microcentrifuge tube. For each littermate pair, one GF animal was conventionalized (CV) using prepared fecal slurry and administered by oral gavage at 10 μl/g body weight. To ensure conventionalization, whiskers and anus were swabbed, and the remaining slurry was painted onto several pieces of food left on the bottom of the animals' cage. CV animals were housed individually throughout the duration of conventionalization with access to food and water *ad libitum*.

IEC Isolation and FACS—After a 2-week conventionalization, both the CV and GF animals were anesthetized using isofluorane, then euthanized by cervical dislocation. The small intestine was removed and divided into 3 equal sections. The proximal and distal 10 cm were considered duodenum and ileum, respectively. The middle section was considered jejunum and used for all studies. Jejunum was flushed with ice-cold PBS to remove the contents, and total IECs were prepared for FACS as previously described (14). IECs were sorted using a Mo-Flo XDP cell sorter (Beckman-Coulter, Fullerton, CA) at the University of North Carolina Flow Cytometry Core Facility using previously described gating parameters (13–15). Conventionally raised age-matched Sox9-EGFP animals were included in each individual sorting experiment and used to set Sox9-EGFP gates. CD31-APC (BioLegend, San Diego, CA), CD45-APC (BioLegend), and annexin-V-APC (Life Technologies), and Sytox-Blue (Life Technologies) staining excluded immune cells, endothelial cells, and apoptotic cells, respectively. Sox9-EGFP cells were then subsequently sorted based on Sox9-EGFP intensity directly into RNA lysis buffer (Norgen Biotek, Thorold, ON, Canada). Additionally, NS IECs were collected for each animal, except one conventionalized mouse (CV314) which did not have enough remaining sample to isolate a NS IEC population. NS IECs were purified by FACS to exclude non-epithelial and dying cells but were not sorted based on Sox9-EGFP intensity. Due to the density of cells, $Sox9^{Neg}$ cells were sorted into cell culture media, then pelleted after sorting by centrifugation. Total RNA was isolated using either the Norgen Total RNA kit ($Sox9^{Neg}$ and NS) or Norgen Single-Cell RNA Purification kit ($Sox9^{High}$, $Sox9^{Low}$, $Sox9^{Sublow}$; Norgen) as per the manufacturer's instructions. Nanodrop 2000 was used to quantify RNA.

mRNA Library Preparation and Sequencing—mRNA se quencing libraries were prepared from 10 ng of total RNA using the Clontech SMARTer Ultra Low Input library preparation kit combined with Nextera XT DNA sample preparation kit (Illumina) by the UNC High Throughput Sequencing Core Facility (as per the Clontech sample preparation guide). Four libraries were randomly pooled per lane and sequenced 100 bp single-end on a HiSeq2000 platform at the UNC High Throughput Sequencing Core Facility. Seven bases were trimmed from the beginning of each read using Trimmomatic (v0.36) (54) to eliminate the remaining SMART adapter sequences, then reads were mapped and aligned to the GENCODE (55–57) mouse transcriptome (vM10) using STAR (v2.4.2a) (58) and SALMON (v0.6.0) (59). Transcript counts were then imported into R (v3.3.1) and were normalized and differential expression of genes quantified using DESeq2 (v1.12.4) (37, 60). Raw sequencing data as well as counts are available through GEO accession GSE81126.

Small RNA Library Preparation and Sequencing—The small RNA sequencing was done at Genome Sequencing Facility of Greehey Children's Cancer Research Institute at University of Texas Health Science Center at San Antonio. Libraries were prepared using an average of 50 ng of total RNA using the TriLink CleanTag Small RNA Ligation kit (TriLink Biotechnologies, San Diego, CA) and the suggested library preparation method. Six to seven libraries were pooled per lane and were sequenced single-end 50× on the HiSeq2000 platform. One GF $Sox9^{Sublow}$ sample failed during sequencing. However, for the remaining samples we received an average of 26.5 million reads per sample. Raw sequencing data and miRNA quantification tables for all samples can be accessed through GEO record GSE81126.

Bioinformatics—Sequencing quality was extremely high as assessed using FASTQC. Reads were trimmed and aligned to the mouse genome (mm9) as previously described (29) with the following modification; only contigs with >1 read alignment were passed into the to Shrimp alignment pipeline. An average of 58.9% of reads mapped to the mouse genome across samples (mapping statistics can be found in supplemental File 1). Due to the large number of reads mapping throughout the genome in GF315 NS IECs, Shrimp failed to align this sample, and it was eliminated from further analysis. Annotated miRNAs with a RPMMM expression threshold of >400 in at least 1 sample were used in further analyses. One aberrant CV $Sox9^{Sublow}$ sample was identified on the basis of poor clustering by PCA and hierarchical clustering analyses and was removed from subsequent analyses.

Enteroid Culture—Jejunum was isolated and flushed with cold PBS (Gibco catalog #14190-144, ThermoFisher Scientific, Waltham, MA), opened, and divided into 6-cm sections. Sections were placed in cold high glucose DMEM and rocked to remove excess fecal matter. Each section was then placed in 3 mM EDTA (cat 46-034-Cl, Corning, Corning, NY) diluted in PBS and rocked at 4 °C for 15 min. The luminal side of the tissue was gently scraped to remove villi and placed into fresh 3 mM EDTA/PBS and rocked an additional 30 min at 4 °C. Sections were shaken for 2 min in ice-cold PBS to remove crypts then filtered through a 70-μm cell strainer and counted. Crypts were resuspended into Reduced Growth Factor Matrigel (catalog #356230, BD Biosciences). Advanced DMEM/F-12 (Gibco, ThermoFisher) supplemented with GlutaMAX (Gibco catalog #35050-061, ThermoFisher), Pen/Strep (Gibco catalog #15140, ThermoFisher), HEPES (Gibco catalog #15630-080, ThermoFisher), 1× N2 supplement (Gibco catalog #17502-048, ThermoFisher), 1 ng/μl EGF (catalog #2028-EG, R&D Systems, Minneapolis, MN), 2 ng/μl Noggin (catalog #250-38, PeproTech, Rocky Hill, NJ), 10 ng/μl murine R-spondin (catalog #3474-RS-050, R&D Systems), and Y27632 (catalog #ALX-270-333-M025, Enzo Life Sciences, Farmingdale, NY) was added. For 48-well plates, 400 crypts were added to 10 μl of Matrigel, and 250 μl of media were added to each well. For 96-well plates, 250 crypts were added to 5 μl of Matrigel, and 125 μl of media were added to each well. Either the media or Matrigel was supplemented with PBS or an equal volume of LNA. For miRNA studies, LNAs were added at 500 nM and include miRCURY LNA Power Inhibitor against miR-375-3p (catalog #4101397,

Exiqon, Woburn, MA) or Negative Control A (catalog #199006, Exiqon). For studies knocking down EGFP, a custom LNA long RNA Standard GapmeR was designed to target EGFP (Exiqon, Design ID: 590367-1), and Negative Control A Gapmer (Exiqon, catalog #300610) was used in concentrations ranging from 500 nM to 5 μM. For EGFP knockdown studies, Lgr5-EGFP$^+$ crypts were identified at day 0 for followup analyses. Enteroids were counted at day 1, and bud formation was assessed at day 4 and day 8 using an Olympus IX83 Inverted Microscope fixed with a live imaging incubator. Images of EGFP$^+$ enteroids were take every 2 days. Media were supplemented with half the original starting concentration of LNA or PBS when changed at day 4, and growth factors were supplemented every other day. Enteroids were harvested at day 8, and RNA was isolated using the Norgen Total RNA isolation kits as per manufacturer's instructions.

Whole Mount Staining of Enteroids—For whole mount staining, enteroids were fixed in 2% paraformaldehyde, then permeabilized using 0.5% Triton X-100 (Sigma) diluted in PBS. Enteroids were blocked using 10% normal goat serum diluted in our immunofluorescence buffer, which consisted of 0.1% bovine serum albumin (Sigma), 0.2% Triton X-100, and 0.05% Tween 20 (Sigma) in PBS. Then, enteroids were stained using antibodies against and Ki67 (ab15580, 1:250, Abcam, Cambridge, MA) diluted in immunofluorescence buffer. Nuclear staining was done using Hoechst 33342 (1:5000, catalog #H3570, ThermoFisher) diluted in immunofluorescence buffer. Confocal imaging was performed at the UNC Microscopy Core Facility on a Zeiss CLSM 710 Spectral Confocal Laser Scanning Microscope.

Analysis of Enteroid Area—At day 8, a z-stack of 4× bright field images capturing the entire well was taken every 10 μm throughout the Matrigel patty. Each enteroid was measured for area at its maximal projection within the z-stack as an estimation of enteroid size using ImageJ. All enteroids that reached at least 1000 μm^2 within each well were included. Three wells from each condition were analyzed from a single experiment.

Validation of miRNA Expression Levels—miRNA expression in the CV and GF animals was validated by qRT-PCR using Taqman assays (Applied Biosystems, Foster City, CA). Relative quantitative value (RQV) for miRNAs was determined relative to control gene *U6*. Gene expression in the CR-sorted cell populations was determined by qRT-PCR using mouse Taqman assays (Applied Biosystems), and RQV was determined relative to control genes *Gapdh* and *Rps9*.

Linear Model—The model covariates include cell type (T), condition (C), littermate pair (P), and sequencing group (G) as well as an interaction term between cell type and condition (Equation 1).

$$Y_{\text{miR}} = \beta_0 + \beta_T\chi_T + \beta_C\chi_C + \beta_{\text{Interaction}}\chi_T \times \chi_C + \beta_P\chi_P + \beta_G\chi_G + \epsilon_{\text{miR}} \quad \text{(Eq. 1)}$$

To determine significance, a multiple testing correction (FDR) was performed on p values for each covariate across all miRNAs.

Author Contributions—B. C. E. P. conceptualized the experiments, conducted the experiments, analyzed and interpreted the data, prepared the figures, and drafted and revised the manuscript. A. T. M. worked with the UNC Gnotobiotic core facility to develop the GF Sox9-EGF model. W. A. P. conducted the experiments and analyzed and interpreted the data. S. D. assisted with experimental design and provided technical advice and assistance with data interpretation. P. K. L. provided assistance with conceptualization and experimental design and contributed to the revision of the manuscript. P. S. obtained funding, provided assistance with conceptualization and experimental design, interpreted the data, supervised the study, and revised the manuscript.

Acknowledgments—We thank R. Eric Blue for help in developing the GF Sox9-EGFP resource, Elaine Glenny for critical assistance with the anaerobic chamber and the protocol for conventionalization, Dr. C. Lisa Kurtz, Dr. Emily Moorefield, Dr. Jeanette Baran-Gale, and Dr. Kasia Kedziora for technical assistance and training, Dr. John Rawls, Dr. Scott Magness, Dr. Susan Henning, Dr. Michael Shanahan, and Dr. Ajay Gulati for helpful discussions as well as Felicia Heyward and UNC Flow Cytometry Core Facility, the UNC Gnotobiotic Core Facility, Dr. Zhao Lai and the UTHSCSA Genome Sequencing Facility, and Dr. Bob Bagnell and the UNC Microscopy Services Laboratory for critical services. The UNC Gnotobiotic Core Facility is supported through National Institutes of Health Grants P39DK034987 and P40OD010995.

References

1. Creamer, B., Shorter, R. G., and Bamforth, J. (1961) The turnover and shedding of epithelial cells. *Gut* **2,** 110–118
2. Velasquez-Manoff, M. (2015) Gut microbiome: the peacekeepers. *Nature* **518,** S3–S11
3. Everard, A., and Cani, P. D. (2014) Gut microbiota and GLP-1. *Rev. Endocr. Metab. Disord.* **15,** 189–196
4. Jaladanki, R. N., and Wang, J.-Y. (2011) *Regulation of gastrointestinal mucosal growth* (Granger, D. N., and Granger, J. P., eds) Morgan & Claypool Life Sciences, San Rafael, CA
5. Siciliano, V., Garzilli, I., Fracassi, C., Criscuolo, S., Ventre, S., and di Bernardo, D. (2013) miRNAs confer phenotypic robustness to gene networks by suppressing biological noise. *Nat. Commun.* **4,** 2364
6. McKenna, L. B., Schug, J., Vourekas, A., McKenna, J. B., Bramswig, N. C., Friedman, J. R., and Kaestner, K. H. (2010) MicroRNAs control intestinal epithelial differentiation, architecture, and barrier function. *Gastroenterology* **139,** 1654–1664
7. Biton, M., Levin, A., Slyper, M., Alkalay, I., Horwitz, E., Mor, H., Kredo-Russo, S., Avnit-Sagi, T., Cojocaru, G., Zreik, F., Bentwich, Z., Poy, M. N., Artis, D., Walker, M. D., Hornstein, E., Pikarsky, E., and Ben-Neriah, Y. (2011) Epithelial microRNAs regulate gut mucosal immunity via epithelium-T cell crosstalk. *Nat. Immunol.* **12,** 239–246
8. Wang, D., Xia, M., Yan, X., Li, D., Wang, L., Xu, Y., Jin, T., and Ling, W. (2012) Gut microbiota metabolism of anthocyanin promotes reverse cholesterol transport in mice via repressing miRNA-10b. *Circ. Res.* **111,** 967–981
9. Dalmasso, G., Nguyen, H. T., Yan, Y., Laroui, H., Charania, M. A., Ayyadurai, S., Sitaraman, S. V., and Merlin, D. (2011) Microbiota modulate host gene expression via microRNAs. *PLoS ONE* **6,** e19293
10. Archambaud, C., Sismeiro, O., Toedling, J., Soubigou, G., Bécavin, C., Lechat, P., Lebreton, A., Ciaudo, C., and Cossart, P. (2013) The intestinal microbiota interferes with the microRNA response upon oral *Listeria* infection. *mBio.* **4,** e00707-13
11. Gong, S., Zheng, C., Doughty, M. L., Losos, K., Didkovsky, N., Schambra, U. B., Nowak, N. J., Joyner, A., Leblanc, G., and Hatten, M. E., and Heintz, N. (2003) A gene expression atlas of the central nervous system based on bacterial artificial chromosomes. *Nature* **425,** 917–925

12. Formeister, E. J., Sionas, A. L., Lorance, D. K., Barkley, C. L., Lee, G. H., and Magness, S. T. (2009) Distinct SOX9 levels differentially mark stem/progenitor populations and enteroendocrine cells of the small intestine epithelium. *Am. J. Physiol. Gastrointest. Liver Physiol.* **296,** G1108–G1118
13. Gracz, A. D., Ramalingam, S., and Magness, S. T. (2010) Sox9 expression marks a subset of CD24-expressing small intestine epithelial stem cells that form organoids *in vitro*. *Am. J. Physiol. Gastrointest. Liver Physiol.* **298,** G590–G600
14. Van Landeghem, L., Santoro, M. A., Krebs, A. E., Mah, A. T., Dehmer, J. J., Gracz, A. D., Scull, B. P., McNaughton, K., Magness, S. T., and Lund, P. K. (2012) Activation of two distinct Sox9-EGFP-expressing intestinal stem cell populations during crypt regeneration after irradiation. *Am. J. Physiol. Gastrointest. Liver Physiol.* **302,** G1111–G1132
15. Mah, A. T., Van Landeghem, L., Gavin, H. E., Magness, S. T., and Lund, P. K. (2014) Impact of diet-induced obesity on intestinal stem cells: hyperproliferation but impaired intrinsic function that requires insulin/IGF1. *Endocrinology* **155,** 3302–3314
16. Andres, S. F., Simmons, J. G., Mah, A. T., Santoro, M. A., Van Landeghem, L., and Lund, P. K. (2013) Insulin receptor isoform switching in intestinal stem cells, progenitors, differentiated lineages and tumors: evidence that IR-B limits proliferation. *J. Cell Sci.* **126,** 5645–5656
17. Roche, K. C., Gracz, A. D., Liu, X. F., Newton, V., Akiyama, H., and Magness, S. T. (2015) SOX9 maintains reserve stem cells and preserves radioresistance in mouse small intestine. *Gastroenterology* **149,** 1553–1563.e10
18. El Aidy, S., van Baarlen, P., Derrien, M., Lindenbergh-Kortleve, D. J., Hooiveld, G., Levenez, F., Doré, J., Dekker, J., Samsom, J. N., Nieuwenhuis, E. E., and Kleerebezem, M. (2012) Temporal and spatial interplay of microbiota and intestinal mucosa drive establishment of immune homeostasis in conventionalized mice. *Mucosal Immunol.* **5,** 567–579
19. Camp, J. G., Frank, C. L., Lickwar, C. R., Guturu, H., Rube, T., Wenger, A. M., Chen, J., Bejerano, G., Crawford, G. E., and Rawls, J. F. (2014) Microbiota modulate transcription in the intestinal epithelium without remodeling the accessible chromatin landscape. *Genome Res.* **24,** 1504–1516
20. El Aidy, S., Merrifield, C. A., Derrien, M., van Baarlen, P., Hooiveld, G., Levenez, F., Doré, J., Dekker, J., Holmes, E., Claus, S. P., Reijngoud, D.-J., and Kleerebezem, M. (2013) The gut microbiota elicits a profound metabolic reorientation in the mouse jejunal mucosa during conventionalisation. *Gut* **62,** 1306–1314
21. Uribe, A., Alam, M., Johansson, O., Midtvedt, T., and Theodorsson, E. (1994) Microflora modulates endocrine cells in the gastrointestinal mucosa of the rat. *Gastroenterology* **107,** 1259–1269
22. Sharma, R., and Schumacher, U. (1996) The diet and gut microflora influence the distribution of enteroendocrine cells in the rat intestine. *Experientia* **52,** 664–670
23. Sommer, F., and Bäckhed, F. (2013) The gut microbiota: masters of host development and physiology. *Nat. Rev. Microbiol.* **11,** 227–238
24. Ishikawa, K., Satoh, Y., Tanaka, H., and Ono, K. (1986) Influence of conventionalization on small-intestinal mucosa of germ-free Wistar rats: quantitative light microscopic observations. *Acta Anat.* **127,** 296–302
25. Guenet, J. L., Sacquet, E., Gueneau, G., and Meslin, J. C. (1970) Action de la microflore totale du rat sur i'activité mitotique des cryptes de lieberkühn. *C. R. Acad. Sci. (Paris)* **270,** 3087–3090
26. Gene Ontology Consortium. (2015) Gene Ontology Consortium: going forward. *Nucleic Acids Res.* **43,** D1049–D1056
27. Ashburner, M., Ball, C. A., Blake, J. A., Botstein, D., Butler, H., Cherry, J. M., Davis, A. P., Dolinski, K., Dwight, S. S., Eppig, J. T., Harris, M. A., Hill, D. P., Issel-Tarver, L., Kasarskis, A., Lewis, S., Matese, J. C., Richardson, J. E., Ringwald, M., Rubin, G. M., and Sherlock, G. (2000) Gene ontology: tool for the unification of biology. The Gene Ontology Consortium. *Nat. Genet.* **25,** 25–29
28. Chen, E. Y., Tan, C. M., Kou, Y., Duan, Q., Wang, Z., Meirelles, G. V., Clark, N. R., and Ma'ayan, A. (2013) Enrichr: interactive and collaborative HTML5 gene list enrichment analysis tool. *BMC Bioinformatics* **14,** 128
29. Baran-Gale, J., Fannin, E. E., Kurtz, C. L., and Sethupathy, P. (2013) Beta cell 5′-shifted isomiRs are candidate regulatory hubs in type 2 diabetes. *PLoS ONE* **8,** e73240
30. Hino, K., Tsuchiya, K., Fukao, T., Kiga, K., Okamoto, R., Kanai, T., and Watanabe, M. (2008) Inducible expression of microRNA-194 is regulated by HNF-1 during intestinal epithelial cell differentiation. *RNA* **14,** 1433–1442
31. Melkman-Zehavi, T., Oren, R., Kredo-Russo, S., Shapira, T., Mandelbaum, A. D., Rivkin, N., Nir, T., Lennox, K. A., Behlke, M. A., Dor, Y., and Hornstein, E. (2011) miRNAs control insulin content in pancreatic β-cells via downregulation of transcriptional repressors. *EMBO J.* **30,** 835–845
32. Grün, D., Lyubimova, A., Kester, L., Wiebrands, K., Basak, O., Sasaki, N., Clevers, H., and van Oudenaarden, A. (2015) Single-cell messenger RNA sequencing reveals rare intestinal cell types. *Nature* **525,** 251–255
33. Stein, C. A., Hansen, J. B., Lai, J., Wu, S., Voskresenskiy, A., Høg, A., Worm, J., Hedtjärn, M., Souleimanian, N., Miller, P., Soifer, H. S., Castanotto, D., Benimetskaya, L., Ørum, H., and Koch, T. (2010) Efficient gene silencing by delivery of locked nucleic acid antisense oligonucleotides, unassisted by transfection reagents. *Nucleic Acids Res.* **38,** e3–e3
34. Knudsen, L. A., Petersen, N., Schwartz, T. W., and Egerod, K. L. (2015) The microRNA repertoire in enteroendocrine cells: Identification of miR-375 as a potential regulator of the enteroendocrine lineage. *Endocrinology* **156,** 3971–3983
35. Fuller, M. K., Faulk, D. M., Sundaram, N., Shroyer, N. F., Henning, S. J., and Helmrath, M. A. (2012) Intestinal crypts reproducibly expand in culture. *J. Surg. Res.* **178,** 48–54
36. Seiler, K. M., Schenhals, E. L., von Furstenberg, R. J., Allena, B. K., Smith, B. J., Scaria, D., Bresler, M. N., Dekaney, C. M., and Henning, S. J. (2015) Tissue underlying the intestinal epithelium elicits proliferation of intestinal stem cells following cytotoxic damage. *Cell Tissue Res.* **361,** 427–438
37. Love, M. I., Huber, W., and Anders, S. (2014) Moderated estimation of fold change and dispersion for RNA-seq data with DESeq2. *Genome Biol.* **15,** 550
38. Yan, J.-W., Lin, J.-S., and He, X.-X. (2014) The emerging role of miR-375 in cancer. *Int. J. Cancer* **135,** 1011–1018
39. Wang, Y., Huang, C., Reddy Chintagari, N., Bhaskaran, M., Weng, T., Guo, Y., Xiao, X., and Liu, L. (2013) miR-375 regulates rat alveolar epithelial cell trans-differentiation by inhibiting Wnt/−catenin pathway. *Nucleic Acids Res.* **41,** 3833–3844
40. Zhang, Z.-W., Men, T., Feng, R.-C., Li, Y.-C., Zhou, D., and Teng, C.-B. (2013) miR-375 inhibits proliferation of mouse pancreatic progenitor cells by targeting YAP1. *Cell. Physiol. Biochem.* **32,** 1808–1817
41. Nezami, B. G., Mwangi, S. M., Lee, J. E., Jeppsson, S., Anitha, M., Yarandi, S. S., Farris, A. B., 3rd, and Srinivasan, S. (2014) MicroRNA 375 mediates palmitate-induced enteric neuronal damage and high-fat diet-induced delayed intestinal transit in mice. *Gastroenterology* **146,** 473–483.e3
42. Poy, M. N., Hausser, J., Trajkovski, M., Braun, M., Collins, S., Rorsman, P., Zavolan, M., and Stoffel, M. (2009) miR-375 maintains normal pancreatic alpha- and beta-cell mass. *Proc. Natl. Acad. Sci. U.S.A.* **106,** 5813–5818
43. Nathan, G., Kredo-Russo, S., Geiger, T., Lenz, A., Kaspi, H., Hornstein, E., and Efrat, S. (2015) MiR-375 promotes redifferentiation of adult human β cells expanded *in vitro*. *PLoS ONE* **10,** e0122108
44. Poy, M. N., Eliasson, L., Krutzfeldt, J., Kuwajima, S., Ma, X., Macdonald, P. E., Pfeffer, S., Tuschl, T., Rajewsky, N., Rorsman, P., and Stoffel, M. (2004) A pancreatic islet-specific microRNA regulates insulin secretion. *Nature* **432,** 226–230
45. Walker, E. M., Thompson, C. A., and Battle, M. A. (2014) GATA4 and GATA6 regulate intestinal epithelial cytodifferentiation during development. *Dev. Biol.* **392,** 283–294
46. Whissell, G., Montagni, E., Martinelli, P., Hernando-Momblona, X., Sevillano, M., Jung, P., Cortina, C., Calon, A., Abuli, A., Castells, A., Castellvi-Bel, S., Nacht, A. S., Sancho, E., Stephan-Otto Attolini, C., Vicent, G. P., Real, F. X., and Batlle, E. (2014) The transcription factor GATA6 enables self-renewal of colon adenoma stem cells by repressing BMP gene expression. *Nat. Cell Biol.* **16,** 695–707
47. Pédron, T., Mulet, C., Dauga, C., Frangeul, L., Chervaux, C., Grompone, G., and Sansonetti, P. J. (2012) A crypt-specific core microbiota resides in the mouse colon. *mBio* **3,** e00116-12

48. Peck, B. C., Sincavage, J., Feinstein, S., Mah, A. T., Simmons, J. G., Lund, P. K., and Sethupathy, P. (2016) miR-30 family controls proliferation and differentiation of intestinal epithelial cell models by directing a broad gene expression program that includes SOX9 and the ubiquitin ligase pathway. *J. Biol. Chem.* **291,** 15975–15984
49. Sasabe, J., Miyoshi, Y., Rakoff-Nahoum, S., Zhang, T., Mita, M., Davis, B. M., Hamase, K., and Waldor, M. K. (2016) Interplay between microbial d-amino acids and host d-amino acid oxidase modifies murine mucosal defence and gut microbiota. *Nat. Microbiol.* **1,** 16125
50. Cobo, E. R., Kissoon-Singh, V., Moreau, F., and Chadee, K. (2015) Colonic MUC2 mucin regulates the expression and antimicrobial activity of β-defensin 2. *Mucosal Immunol.* **8,** 1360–1372
51. Salzman, N. H., Hung, K., Haribhai, D., Chu, H., Karlsson-Sjöberg, J., Amir, E., Teggatz, P., Barman, M., Hayward, M., Eastwood, D., Stoel, M., Zhou, Y., Sodergren, E., Weinstock, G. M., Bevins, C. L., Williams, C. B., and Bos, N. A. (2010) Enteric defensins are essential regulators of intestinal microbial ecology. *Nat. Immunol.* **11,** 76–83
52. van Niel, G., Raposo, G., Candalh, C., Boussac, M., Hershberg, R., Cerf-Bensussan, N., and Heyman, M. (2001) Intestinal epithelial cells secrete exosome-like vesicles. *Gastroenterology* **121,** 337–349
53. Liu, S., da Cunha, A. P., Rezende, R. M., Cialic, R., Wei, Z., Bry, L., Comstock, L. E., Gandhi, R., and Weiner, H. L. (2016) The host shapes the gut microbiota via fecal microRNA. *Cell Host Microbe* **19,** 32–43
54. Bolger, A. M., Lohse, M., and Usadel, B. (2014) Trimmomatic: a flexible trimmer for Illumina sequence data. *Bioinformatics* **30,** 2114–2120
55. Mudge, J. M., and Harrow, J. (2015) Creating reference gene annotation for the mouse C57BL6/J genome assembly. *Mamm. Genome* **26,** 366–378
56. Harrow, J., Denoeud, F., Frankish, A., Reymond, A., Chen, C.-K., Chrast, J., Lagarde, J., Gilbert, J. G., Storey, R., Swarbreck, D., Rossier, C., Ucla, C., Hubbard, T., Antonarakis, S. E., and Guigo, R. (2006) GENCODE: producing a reference annotation for ENCODE. *Genome Biol.* **7,** S4.1–9
57. Harrow, J., Frankish, A., Gonzalez, J. M., Tapanari, E., Diekhans, M., Kokocinski, F., Aken, B. L., Barrell, D., Zadissa, A., Searle, S., Barnes, I., Bignell, A., Boychenko, V., Hunt, T., Kay, M., *et al.* (2012) GENCODE: the reference human genome annotation for The ENCODE Project. *Genome Res.* **22,** 1760–1774
58. Dobin, A., Davis, C. A., Schlesinger, F., Drenkow, J., Zaleski, C., Jha, S., Batut, P., Chaisson, M., and Gingeras, T. R. (2013) STAR: ultrafast universal RNA-seq aligner. *Bioinformatics* **29,** 15–21
59. Patro, R., Duggal, G., and Kingsford, C. (2015) Salmon: Accurate, versatile and ultrafast quantification from rna-seq data using lightweight alignment. *bioRxiv* 10.1101/021592
60. Anders, S., and Huber, W. (2010) Differential expression analysis for sequence count data. *Genome Biol.* **11,** R106 .